

LAND USE CLASSIFICATION BASED ON OBJECT-ORIENTED ANALYSIS - A SHIHMEN RESERVOIR CASE

Kuan-Tsung Chang^{*1}, Jin-King Liu², Edward Wang³, Zhu-Yi Wang⁴ and Yan-Xiang Lin⁴

¹Assistant Professor, Department of Civil Engineering and Environmental Informatics, Minghsin University of Science and Technology; Tel:+886-3-5593142 ext. 3282, E-mail:ktchang1216@gmail.com

²CEO, LIDAR Technology Co., Ltd; Tel:+886-3-6589495, E-mail:jkliu@lidar.com.tw

³Associate Professor, Department of Civil Engineering and Environmental Informatics, Minghsin University of Science and Technology, E-mail:ewang@must.edu.tw

⁴Graduate Student, Department of Civil Engineering and Environmental Informatics, Minghsin University of Science and Technology; Tel:+886-3-5593142 ext. 3282, E-mail:ricebug12@gmail.com

KEY WORDS: Land Use, Classification, Object-Oriented Analysis, Interpretation Keys

ABSTRACT: Hillside region accounts for 73.6% of the land in Taiwan. The mountain region consists of high mountain valley of deep and faults-knit environment, fragile geological, abrupt slopes, and steep rivers. With the rapid development in recent years, there has been not only great change in land use, but the destruction of the natural environment, the improper use of soil and water resources also. It is prudent to effectively build and renew the existing land use information as soon as possible. Among various land use status investigation and monitoring technology, the remote sensing has the advantages in getting data covering wide-range and in richness of spectral and spatial information. Currently, the application of remote sensing and the geographic information system in assessing the soil and water conservation and management plays a vital role. The Shihmen Reservoir and its catchment area is the main water supply resource across areas including, the Taoyuan County, parts of Hsinchu County. The aboriginal reservations within this area have been developed for resort and need to be conserved. The objective of this study is to apply SPOT 5 satellite images and digital terrain data to develop an automatic land use classification method. The second land use investigation result of Taiwan in 2008 by the Ministry of the Interior is assumed as the ground truth. An object-based analysis was performed for the land use classification experiment, and accuracy assessment for interpretation also given.

The preliminary test results showed that in landslide interpretation, object-based methods were significantly better than pixel-based methods. It is proved that the object-based method can raise efficiency and accuracy of land use automatic classification. In this study, an object-oriented land use classification is established and this method gives additional benefit in summarizing the interpretation keys for the land use investigation.

1. INTRODUCTION

Land use is the human use of land. Land use involves the management and modification of natural environment or wilderness into built environment such as fields, pastures, and settlements. It has also been defined as "the arrangements, activities and inputs people undertake in a certain land cover type to produce, change or maintain it" (Wikipedia). Taiwan has a land area of 36000m², 26.68% of which are covered by plain region, whereas 27.31% of which are hilly and 46.01% are mountainous. By official definition for the purpose of land conservation management, hilly lands refer to the area between 100 m and 1000 m AMSL or the area under 100 m but with a slope more than 5%. Mountainous lands refer to the area with an altitude above 1000 m AMSL (Liu et al., 2009). Peoples can make use of limited land area. However, sustainable highly economic growth drive urbanization and land development making changes in land use types more frequently. In the Shihmen reservoir and its catchment, there are some lands used for fruit, tea planting, and hostel. If the real-time status of land use can be grasped, it closely related to the regional planning of water resource, disaster prevention, and conservation. There are three kinds of commonly used survey methods for the status survey of land use, means ground survey, aerial or space-borne survey (Lillesand et al., 2004; Liu, et al., 2009), or a combination of these methods (Gali, et al., 2008). Ground surveys are highly accurate, although slow. When inventory area is very large, accessibility is generally low. Therefore, it is impossible to make the survey in near real-time or to achieve complete huge coverage. This is also the used method in Taiwan for the first time land use census from 1993 to 1995. (Huang et al., 2007) Photographic or image interpretation approaches do not suffer accessibility problems. Aerial photography is a commonly chosen option, used extensively to characterize its geometric boundary and its attributes for each land category, particularly with high spatial resolution stereoscopic images. This approach can resolve and define individual land-use object very clearly. Manually, semi-automatic, and automatic interpretation of photographic

data are all used. Manual interpretation requires well-trained investigators to delineate the land-use objects from stereoscopic images or ortho-rectified images. However, the conventional photo-interpretation is a time-consuming and labor-intensive approach (Lillesand et al., 2004; Huang et al., 2007). With the exception of aerial photography, satellite imagery is useful for collection of data on relevant parameters, including soils, geology, slope, geomorphology, land use, hydrology, rainfall, faults, hot springs and so on. Multispectral images are useful for the classification of lithology, vegetation, and land use. Researchers may use stereo SPOT imagery to perform geo-morphological mapping and terrain classification (Liang, 1997; Hsu et al., 2002; McKean et al., 2005). Automatic classification of land use condition is based on certain criteria and computing algorithms, e.g. image classification methods. The advantage for image classification is the objectiveness of the approach. Several investigators have attempted to identify pattern or objects using pixel-based classification methods, e.g. Maximum Likelihood method (Yang, 2007), Artificial Neural Network methods (Zurada, 1992; Parise, 2001; Barlow et al., 2003; Chang and Liu, 2004), and Support Vector Machine (Zhu and Blumberg, 2002; Foody and Mathur, 2004; Camps-Valls and Bruzzone, 2005). Traditional methods for classification of remote sensing data e.g. Maximum Likelihood method (ML) based on statistical analyses; use a priori statistical information, e.g. a probability distribution. The Hughes Effect requires that increasing the number of data bands impose a need to increase the number of training samples; otherwise, the use of additional bands degrades the performance of the classification criteria. ANNs are both powerful and versatile computational tools for organizing and correlating information in ways that have proven useful for solving certain types of problems that are too complex, too poorly understood, or too resource-intensive to tackle using traditional computational methods. However, the trained network is a black box, whereby the internal workings of the network are unknown, and the derived solution often tends to local extreme values (Bischof et al., 1992). Support Vector Machine (SVM) is a new pattern recognition method, which uses adaptive learning methods. SVM processes high-dimensional data, and has received extensive attention in the field of the remote sensing applications. Some variant SVM methods had been used in land use/cover classification projects. Experimental results from these variant methods demonstrated that the SVM method is more accurate than other pixel-based classification methods (Chen, 2006). By pixel-wise classification, land-use objects can occupy only individual or just a few pixels without forming an outer shape of land use. Moreover, commission and omission errors can further complicate the situation. The pixel-based methods are then required to be replaced with approaches based on objects or segments (Kerle and Martha, 2010).

2. OBJECT-ORIENTED ANALYSIS

Object-oriented analysis (OOA) is inherently more suitable, as it can address the phenomena under study such as land use categories in this case, as that they are “objects”, not “pixels” that have spectral, spatial and contextual characteristics. Subsequently, a region-based segmentation combining a supervised classification method named support vector machine (SVM) are applied to the satellite image to find out an optimal range of feature values to present land-use objects (Research System, Inc., 2010; Chang et al., 2010). The segmentation and SVM approaches implemented in the paper are explained in detailed below.

2.1 Region-based segmentation

Basic task of segmentation algorithms is the merge of image elements based on homogeneity parameters or on the differentiation to neighboring regions (i.e. heterogeneity), respectively. Thus, segmentation methods follow the two strongly correlated principles of neighborhood and similarity of pixel values. Generally the following strategies for partitioning a scene into regions can be applied: Region-based approaches start in image space where the available elements either pixels or already existing regions are tested for similarity against other elements. Concerning the definition of the initial segmentation the procedures of region growing (i.e. bottom-up, i.e. starting with a seed pixel) and region splitting (i.e. top-down, i.e. starting with the entire scene) are distinguished. One disadvantage of the splitting method is that it tends to be over-segmented because a splitting always produces a fixed number of sub-regions (normally: 4) although two or three of them might actually be homogeneous with respect to each other. As a consequence, one can apply an integration of the various methods. Thus, it leads to the split-and-merge algorithm that after a split process, if neighboring regions are similar, they should be remerged again.

To strengthen the automation of segmentation, clustering is adopted for region-based segmentation. The ISOCLUST is an iterative self-organizing unsupervised classifier based on a concept similar to the well-known ISODATA routine of Ball and Hall and cluster routines such as the H-means and K-means procedures (Jain and Dubes, 1988).

2.2 Support Vector Machine

SVM is a relatively new classifier and is based on strong foundations from the broad area of statistical learning theory. Since its inception in early 90s, it has found applications in a wide range of pattern recognition problems, image classification, financial time series prediction, face detection, biomedical signal analysis, medical diagnostics, and data mining (Chapelle et al., 1999; Hwang and Chiang, 2010). Under the basic assumption of the SVM

approach, the training sample is expressed as $\{(x_1, y_1), (x_2, y_2), \dots, (x_n, y_n)\}$ where $x_i \in R^d$ represents an input mode, and $y_j \in \{\pm 1\}$. The optimal decision-making formula is as follows:

$$w^T x_i + b = 0 \quad (1)$$

The weighing vectors w and b is deemed satisfactory once converged.

$$y_i(w^T x_i + b) \geq 1 - \varepsilon_i. \quad (2)$$

The value ε_i is a loose variable existing in a linear, undividable condition. It describes the degree of module deviation under the ideal linear circumstances. The goal of the SVM is to identify a decision support phase where the average error of the training samples is minimized. The optimization equation is therefore derived as follows:

$$\varphi(w, \varepsilon) = \frac{1}{2} w^T w + C \sum_{i=1}^N \varepsilon^i \quad (3)$$

Where C is a positive parameter assigned by the end user. It serves as a penalty for the correctness of the SVM. The C value is used to leverage the probable misinterpretation percentage and the complexity of the algorithm. A converged optimization equation can be derived adopting the Lagrange Multiplication Method:

$$Q(\alpha) = \sum_{i=1}^N \alpha_i - \frac{1}{2} \sum_{i=1}^N \sum_{j=1}^N \alpha_i \alpha_j y_i y_j K(x_i, x_j) \quad (4)$$

Where $K(x_i, x_j)$ is a core function, and $\{\alpha_i\}_{i=1}^N$ is a Lagrange multiplier while Eq. (4) fulfilling the following criteria:

$$\sum_{i=1}^N \alpha_i y_i = 0, \quad 0 \leq \alpha_i \leq C, \quad i = 1, 2, 3, \dots, N \quad (5)$$

3. CASE STUDY

The Shihmen reservoir was built in 1963, it is a major water resource for the Taoyuan area. Its main function of the original design is the supply of agricultural water. The occupied area of reservoir and its catchment is 76340 Ha. Most of the land is hillside terrain between 100 m and 3500 m AMSL. The catchment contains steep slope and geological fracture, besides the whole area belongs to the water quality and quantity protection area. Therefore, lower limits of available land can be realized. (Construction and Planning Agency, 2005, 2009)

This catchment is used as study area in this paper, and the results in the second time national land use census in 2006 is used as the ground truth shown as Figure 1. Now there are nine land-use types in the level one classify of the ground truth as the handling objects. The land-use types and their corresponding code named LCODE shown as Table 1. First of all, the vector map was imported into the ENVI software. Next it was transformed to the regions of interest (ROI) to summarize the value statistic of spectral and geo-morphometric features on the satellite image and digital terrain models, respectively. Then the satellite image can be clustering into some regional objects using the segmentation function, and some objects are selected as training samples for the SVM classifier. Finally, the accuracy assessment of the SVM classification results can be given.

Table 1. The nine land-use types and their LCODE

LCODE	Land-use type
1	Agriculture land
2	Forestry land
3	Transportation land
4	Hydrology land
5	Building-up land
6	Infrastructure land
7	Recreation land
8	Mining land
9	Other

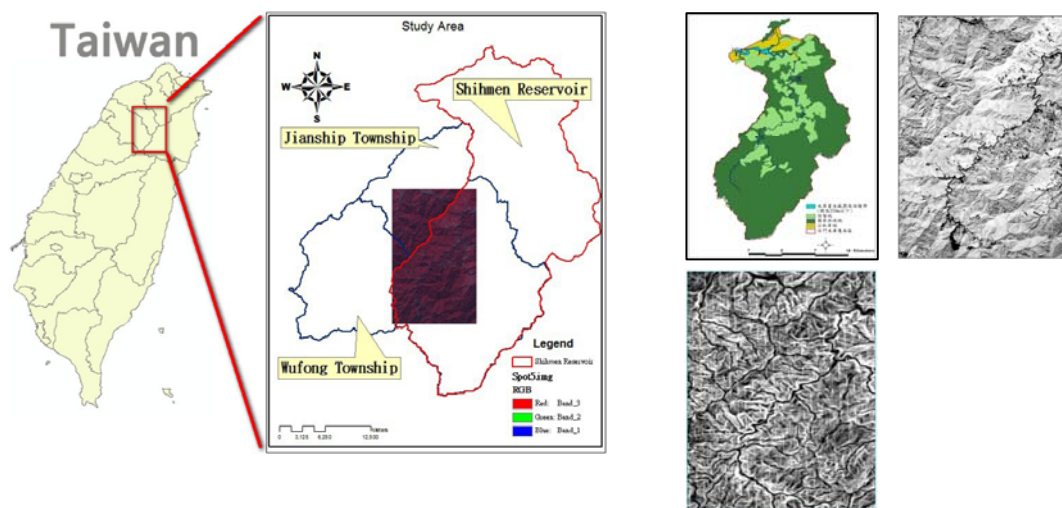


Figure 1. The study area, used data, and ground truth.

4. RESULTS AND ANALYSIS

A SPOT 5 satellite image is used in this study (©SPOT Image Copyright 2010 CNES), the digital value in the R, G, B, and NIR bands, and the NDVI value are generated as the spectral features. And slope feature calculated from the Aster GDEM (The GDEM is downloaded from NASA). According to the above mentioned experimental procedures, the feature statistic for each land-use type shown as Figure 2a-2f. In this figure, the distribution shows that the range of features value for the agriculture type is closely to the range distribution of the forestry land. However, the range of features value for the LCODE 6-9 is large which means the significant features cannot be found for these four land-use types.

Moreover, the experimental results for the object-based land use classification shown as Figure 3-5. As the occupied area ratio of the transportation land (LCODE 3) and the building-up land (LCODE 5) in this study area only is 0.52% and 0.27%, respectively. Adequate training is not easy to select the appropriate samples from the segmented result. Therefore, the classification result for these two land-use types can easily be mistaken for other types. Preliminary visual assessment of object-based classification accuracy is not satisfactory with the purpose of this research. It will be inferred that the lower resolution for the used satellite image and DTM data, the disparity in occupied area ratio for nine land-use types, and the used features is not satisfactory for the land-use interpretation keys.

5. Conclusions and Suggestions

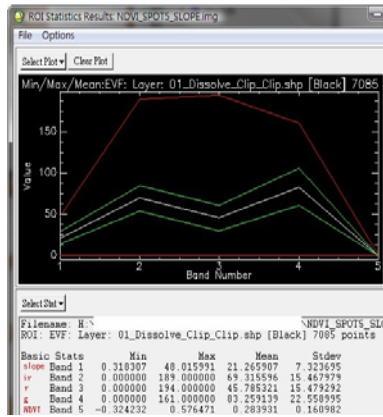
The feature statistic results indicate that the range of features value for the agriculture type is closely to the range distribution of the forestry land. Beside the range of features value for the LCODE 6-9 is large which means the significant features cannot be found for these four land-use types.

The experimental results for the object-based land use classification show that adequate training is not easy to select the appropriate samples for the transportation land and the building-up land owing to small occupied area ratio in the study area. Therefore, the classification result for these two land-use types can easily be mistaken for other types. Preliminary visual assessment of object-based classification accuracy is not satisfactory with the purpose of this research. It will be inferred that the lower resolution for the used satellite image and DTM data, the disparity in occupied area ratio for nine land-use types, and the used features is not satisfactory for the land-use interpretation keys. In the future, more experiments in detail will be considered and given.

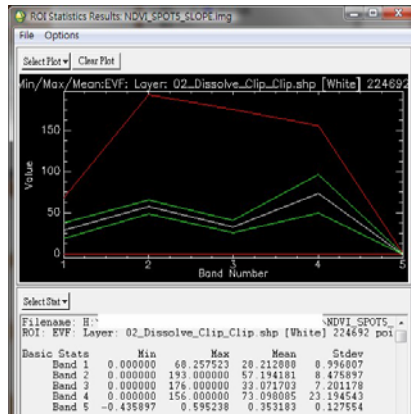
REFERENCES

Barlow, J., Y. Martin, and S. E., Franklin, 2003. Detecting translational landslide scars using segmentation of Landsat ETM+ and DEM data in the northern Cascade Mountains, British Columbia. *Can. J. Remote Sensing*, 29(4) 510-517.

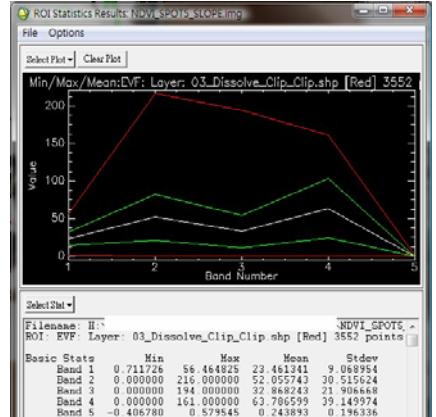
- Bischof, H., W. Schneider, and A. J. Pinz, 1992. Multispectral Classification of Landsat-images Using Neural Networks, *IEEE trans. on Geoscience and Remote Sensing*, 30(3), pp. 482-490.
- Chapelle, O., P. Haffner, and V. N. Vapnik, "Support vector machines for histogram-based image classification," *IEEE Transactions on Neural Networks*, vol. 10 (5), 1999, pp. 1055– 1064.
- Camps-Valls G. and L. Bruzzone, 2005. Kernel-Based Methods for Hyperspectral Image Classification, *IEEE trans. on Geoscience and Remote Sensing*, 43(6), pp. 1351-1362.
- Chang, K T and J K Liu, 2004. Landslide features interpreted by neural network method. In: *The International Archives of the Photogrammetry, Remote Sensing and Spatial Information Sciences*, Istanbul, Turkey, Vol. XX, Part B7, pp.574-579.
- Chang, K. T., J. K. Liu, Y. M. Chang, and C. S. Kao, 2010. An accuracy comparison for the landslide inventory with the BPNN and SVM methods, Gi4DM 2010, Turino, Italy.
- Chen, C. C., 2006. Rice Paddy Identification using the Support Vector Machine and Plausible Neural Network, MSc thesis, Dept. of Civil Eng., NCTU, HsinChu, 109p (in chinese).
- Foody, G. M. and A. Mathur, 2004. A Relative Evaluation of Multiclass Image Classification by Support Vector Machine, *IEEE trans. on Geoscience and Remote Sensing*, 42(6), pp. 1335-1343.
- Galli, M., Ardizzone, F., Cardinali, M., Guzzetti, F., Reichenbach, P., 2008. Comparing landslide inventory maps, *Geomorphology*, 94, 268–289.
- Hwang, J. T. and H. C. Chiang, "The study of high resolution satellite image classification based on Support Vector Machine," *Proc. The 18th International Conference on Geoinformatics*, 2010.
- Hsu, L. D., C. C. Chen, J. P. Tsao, S. Chen, 2002. *Multi-annual SPOT images for monitoring large-scaled landslide*. In: *Proceedings of symposium of annual meeting of Chinese Association of Geographic Information System*. Taichung.
- Huang, Ying-Ting, Kuo-Hsin HSIAO, Jyh-Ching Lin, and Huei-Jhang Su, 2007, A STUDY ON LANDUSE CLASSIFICATION USING ORTHO-RECTIFIED AERIAL PHOTOGRAPHS AND HIGH RESOLUTION SATELLITE IMAGES, *Proceedings of ACRS 2007*.
- Jain, A. K. and R. C. Dubes, "Algorithms for Clustering Data," Prentice Hall, Inc., 1988.
- Kerle, N. and T. R. Martha, "The potential of object-based and cognitive methods for rapid detection and characterisation of landslides," *Proc. Gi4DM 2010*, 2010.
- Liang, L. S., 1997. *Satellite images as applied to the investigation of landslides and hot springs*. MSc. Thesis, Institute for Applied Geology, National Central University.
- Lillesand, T. M., R. W. Kiefer, and J. W. Chipman, 2004. *Remote Sensing and Image Interpretation*, Fifth Edition, John Wiley & Sons, Inc.
- Liu, J. K., K. T. Chang, J. Y. Rau, W. C. Hsu, Z. Y. Liao, C. C. Lau, T. Y. Shih, 2009. *The Geomorphometry of Rainfall-Induced Landslides in Taiwan Obtained by Airborne Lidar and Digital Photography*, Geoscience and Remote Sensing, In-Tech, Inc. (in press)
- LiDAR-derived topographic information for characterizing and differentiating landslide morphology and activity. *Geomorphology*, 73, pp. 131–148. DOI: 10.1016/j.geomorph.2005.07.006.
- McKean, N. F., D. R. Streutker, J. Chadwick, D. J. Glenn, G. D. Thackray, and S. J. Dorsch, 2005. Analysis of Parise, M., 2001. Landslide mapping techniques and their use in the assessment of the landslide hazard. *Physics and Chemistry of the Earth*, 26(9) 697-703, 2001. doi:10.1016/S1464-1917(01)00069-1.
- Research System, Inc., "ENVI Online Help," 2010.
- Research System, Inc., 2010. ENVI Online Help.
- Zhu, G. and D. G. Blumberg, 2002. Classification Using ASTER Data and SVM Algorithms; The Case Study of Beer Sheva, Israel, *Remote Sensing of Environment*, 80(2), pp. 233-240.
- Zurada, J. M., 1992. *Introduction to Artificial Neural Systems*, West Pub. Co., pp.163-248.
- Construction and Planning Agency, 2009. The plan draft for the Shihmen reservoir specific area, Ministry of Interior.
- Construction and Planning Agency, 2005. Land use planning report in the Shihmen reservoir and its catchment, Ministry of Interior.



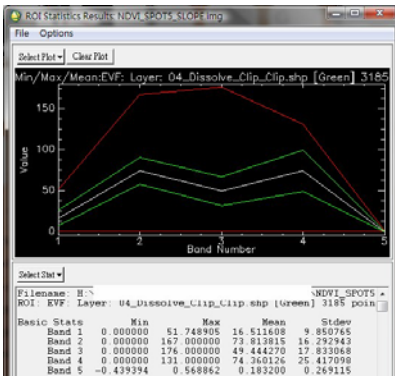
(2a). Agriculture land



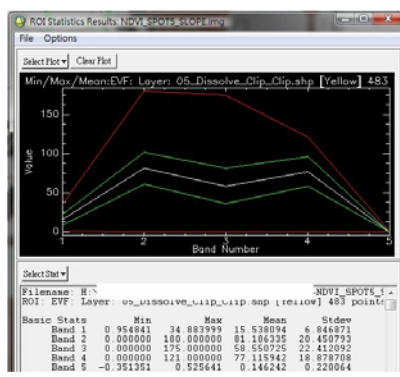
(2b). Forestry land



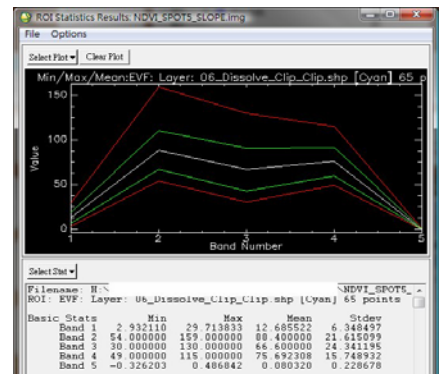
(2c). Transportation land



(2d). Hydrology land



(2e). Building-up land



(2f). Infrastructure land

Figure 2. The feature statistic for each land-use type (other three statistic for LCODE 7-9 omitted)

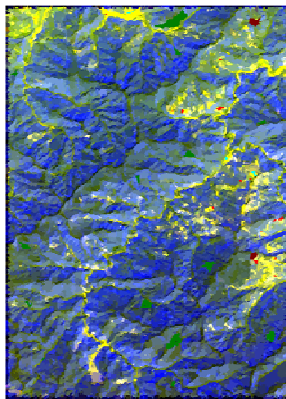


Figure 3. Segmentation and merging result.

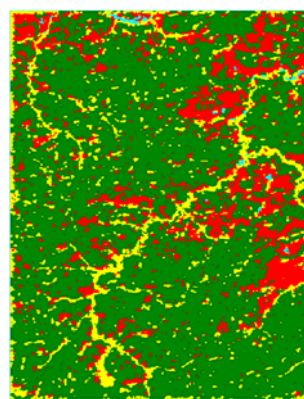


Figure 4. A SVM result

CLASS ID	AREA	LENGTH	COMPACT	CONVECTY	SOLIDITY	REGULARITY	PERIMETER	SLANTW
Category 1	15930	30989725	0.9743	1.50428	0.22811	0.84154	0.86964	1
Category 2	1460940	897368007	0.96261	1.554823	0.84417	0.46197	0.80235	15
Category 3	7590	86.11448	0.92193	1.0640	0.80472	0.60899	0.84738	14
Category 4	8870	184.70264	0.71987	1.58174	0.70949	0.52826	0.83380	13
Category 5	1295	40.91088	0.73987	1	1	0.54848	0.72433	12
Category 6	3003	60.19073	0.8980	1.14266	0.71303	0.37887	0.64875	11
Category 7	8180	471.24018	0.71390	1.88889	0.81833	0.47473	0.69382	10
Category 8	6990	1244.8768	0.73752	1.18835	0.67113	0.88838	0.82488	42
Category 9	5483	386.73869	0.82703	1	1	0.42442	0.81324	9
Category 10	18970	284.12375	0.14335	1.22982	0.88898	0.14786	0.80264	16
Category 11	6700	36	0.24674	1.06789	0.877	0.53836	0.83389	17
Category 12	3770	78.94411	0.90770	1	1	0.48092	0.87839	18
Category 13	12880	481.94811	0.78977	1	1	0.48202	0.86893	19
Category 14	12880	25.848284	0.14488	1.53212	0.62890	0.18878	0.82829	18
Category 15	3003	40	0.24674	1	1	0.53836	0.84134	10
Category 16	11280	514.82818	0.71348	1.88889	0.84843	0.88887	0.81323	15
Category 17	5280	1481.32815	0.71311	1.274	0.88848	0.348	0.82488	11
Category 18	12880	40	0.24674	1.06789	0.71312	0.84843	0.84134	14

Figure 5. The features statistic of each interpreted object